J Mater Sci (2010) 45:1830–1836
DOI 10.1007/s10853-009-4166-4

Microstructure and grindability of as-cast Ti–Sn alloys

Hsueh-Chuan Hsu · Hsi-Chen Lin · Shih-Ching Wu · Yu-Sheng Hong · Wen-Fu Ho

Received: 23 July 2009 / Accepted: 24 December 2009 / Published online: 12 January 2010

Abstract In this study, the structure, microhardness, and grindability of a series of binary Ti–Sn alloys with tin contents ranging from 1 to 30 wt% were investigated. Commercially pure titanium (c.p. Ti) was used as a control. The experimental results indicated that all the Ti–Sn alloys showed hcp α structure, and the hardness values of the Ti–Sn alloys increased with greater Sn contents, ranging from 246 HV (Ti–1Sn) to 357 HV (Ti–30Sn). Among these Ti–Sn alloys, the alloy with 30 wt% Sn content showed the highest hardness value. The grindability of each metal was found to be largely dependent on the grinding conditions. The addition of Sn to c.p. Ti did contribute to improving the grindability of c.p. Ti. The Ti–Sn alloys with a higher Sn concentration could be ground more readily. The grinding rate of the Ti–20Sn alloy at 1200 m/min was about 2.8 times higher than that of c.p. Ti. Additionally, the grinding ratios of the Ti–10Sn, Ti–20Sn, and Ti–30Sn alloys at 1200 m/min were about 2.8, 2.7, and 3.4 times that of c.p. Ti, respectively. Our research suggests that the Ti–Sn alloys with Sn contents of 10 wt% and greater developed here are good candidates for machining by the CAD/CAM method.

H.-C. Hsu · H.-C. Lin · S.-C. Wu
Department of Dental Laboratory Technology, Central Taiwan University of Science and Technology, Taichung, Taiwan, ROC

H.-C. Hsu · S.-C. Wu
Institute of Biomedical Engineering and Material Science, Central Taiwan University of Science and Technology, Taichung, Taiwan, ROC

Y.-S. Hong
Department of Mechanical and Automation Engineering, Da-Yeh University, Changhua, Taiwan, ROC

W.-F. Ho (✉)
Department of Materials Science and Engineering, Da-Yeh University, 168 University Road, Dacun, Changhua 51591, Taiwan, ROC
e-mail: fujii@mail.dyu.edu.tw

Introduction

Recently, commercially pure titanium (c.p. Ti) and its alloys have been increasingly used as implants and prostheses due to their excellent biocompatibility, high strength to weight ratio, corrosion-resistance, and low cost [1]. However, the strength of c.p. Ti is inadequate for dental prostheses requiring comparatively high strength, such as partial dentures, bridges, and implants [2]. Alloying titanium is one method for improving its properties.

Many titanium alloys have been developed for dental use, and their properties have been widely studied [3–5], to improve the strength and castability of pure titanium. Casting metals is not the only way to fabricate dental prostheses. Recently, the CAD/CAM (computer-aided design and manufacturing) method has demonstrated notable advancement over casting technology [6]. CAD/CAM technology produces restorations in one office visit. After the tooth is prepared, the preparation is optically scanned and the image is computerized. The restoration is then machined by a computer-controlled machine [7]. CAD/CAM systems provide an alternative method to produce metal, ceramic, or composite restorations, without the need for any procedures that require two or more patient appointments. However, the poor machinability (ease of cutting or grinding) of titanium is an obstacle to practical dental applications. If current titanium prostheses are fabricated by CAD/CAM, the tool life is short and the processing time is long [3]. Therefore, further development of new dental materials suitable for efficient machining is

required. Much effort continues to be devoted to the study of new machining-appropriate dental materials, such as Ti–Au [2], Ti–Cu [8], Ti–Nb [9], Ti–Hf [10], Ti–Cr [11], Ti–5Cr–Fe [12], Ti–Zr [13], and Ti–10Zr–X (X = Nb, Mo, Cr or Fe) [14]. Additionally, grinding is essentially the same process as cutting on a microscopic scale, and evaluating the grindability of a metal can be a guide to evaluating the ease of cutting. Moreover, cutting and grinding are not only the most commonly employed operations in rapidly advancing dental CAD/CAM systems but also essential processes in dental laboratories. As a result, the ease of the CAD/CAM process by using the grindability (grinding rate and grinding ratio) was evaluated in this study.

Among various titanium alloys, Ti–6Al–4V is the most commonly used because of its superior physical and mechanical properties in comparison to c.p. Ti [4]. However, there has been speculation that the release of Al and V ions from the alloy might cause certain long-term health problems [15, 16]. For a metal to be used in a dental restoration, it should be biocompatible so that it does not cause toxicological or allergic reactions. Therefore, caution should be exercised when alloying elements are added. For example, vanadium exhibits high cytotoxicity [17], aluminum may induce senile dementia [17], and nickel has been shown to possess some bio-toxicity [18]. However, tin (Sn) is known to be safe for use as an alloying element with titanium because it is nontoxic and nonallergic [19]. Sn can also be used to strengthen Ti alloys [20]. In our previous research [21], a series of binary Ti–Sn alloys was developed which showed favorable mechanical properties. These alloys can also be used as a metal for dental casting. In this study, the microhardness and grindability of a series of binary Ti–Sn alloys with Sn contents ranging from 1 to 30 wt% were investigated, with the aim of developing a dental titanium alloy with better machinability than unalloyed titanium.

Materials and methods

The materials used in this study included c.p. Ti, Ti–1Sn, Ti–5Sn, Ti–10Sn, Ti–20Sn, and Ti–30Sn alloys (in wt%). All the materials were prepared from raw titanium (99.8% pure; Ultimate Materials Technology, Taiwan), Sn (99.95% pure; Ultimate Materials Technology, Taiwan) by using a commercial arc-melting vacuum-pressure-type casting system (Castmatic, Iwatani Corp., Japan). The processing details of the alloys were reported in our previous work [21].

The cast alloys were sectioned by using a Buehler Isomet low-speed diamond saw to obtain specimens (10.0 × 10.0 × 1.0 mm) for analysis of X-ray diffraction (XRD), microstructural examination, and measuring microhardness. The surfaces of the alloys for microstructural study were mechanically polished by a standard metallographic procedure to a final level of 0.3 μm alumina powder and subsequently etched in a solution of water, nitric acid, and hydrofluoric acid (80:15:5 in volume). The microstructure of the etched alloys was examined by using an optical microscope (BH2, Olympus, Japan). X-ray diffraction for phase analysis was conducted by using a diffractometer (XRD-6000, Shimadzu, Japan) operating at 30 kV and 30 mA. This study also used Ni-filtered CuKα radiation. The respective phases were identified by matching each characteristic peak with the Joint Committee on Powder Diffraction Standards files. The microhardness of the polished alloys was measured by using a microhardness tester (MVK-E3, Mitutoyo, Japan) at 100 gm for 15 s. The microhardness values were obtained from three castings on which at least 15 randomly chosen indentations were measured and averaged.

The method used by several researchers [2, 8–10, 22, 23] in previous studies was adopted to evaluate grindability in this study. A silicon carbide (SiC) wheel (G11, Shofu, Kyoto, Japan), 13.1 mm in diameter and 1.75 mm in thickness, on an electric dental handpiece (Ultimate 500, NSK Nakanishi Inc., Japan) was used to grind the specimens (3.0 × 8.0 × 30.0 mm). By applying a force of 100 gf, the 8.0-mm cross section of the specimens was ground for 1 min at one of the four circumferential speeds (500, 750, 1000, or 1200 m/min). Each specimen was placed on the testing apparatus referred to in a previous study by Ohkubo et al. [23] so that the edge of the wheel contacted one of the sidewalls of the rectangular specimen at 90°. The specimens and wheels were kept in a closed compartment during grinding so that the majority of the metal chips generated could be collected.

The amount of metal removed (mm^3) per minute was calculated from the density, previously measured by using Archimedes' principle [23], and the weight loss of the specimen. A new wheel was applied for every test. The diameter and weight of each wheel were measured before and after grinding. The grindability was evaluated by the grinding rate and grinding ratio. The grinding rate was determined by the volume of metal removed per minute of grinding, and the grinding ratio was determined by the volume ratio of metal removed compared to the wheel material lost [grinding ratio = (amount of metal removed)/(amount of wheel lost)]. The wheel volume loss was calculated by measuring the diameter of each wheel before and after testing. The grinding rate represents ease of metal removal; whereas, the grinding ratio is a measure of wheel life [10]. Three specimens were used to evaluate the grindability of each alloy, for which the test was performed twice per specimen at each grinding speed. All the results in this study were analyzed with ANOVA and Duncan's multiple comparison test at a $p < 0.05$ level.

After testing, the ground surfaces of the metals were observed by using optical microscopy (BH2, Olympus, Japan). The appearance of the chips resulting from the metal grinding was examined by using scanning electron microscopy (SEM; S-3000 N, Hitachi, Japan). In this study, the experimental alloys were fabricated by using a graphite mold instead of a dental investment mold, a detail which should not affect the outcome. According to the results obtained by Ohkubo et al. [23], there was no appreciable difference in the grindability between c.p. Ti with and without α-cases when a SiC wheel was used. Moreover, most studies were performed for specimens whose α-case layer was totally removed [2, 8–10]. The thickness of the α-case depends on experimental factors such as cooling rate, casting geometry, amount of oxygen at the mold/casting interface, extent of the reaction with the mold material, etc. Koike et al. [24] evaluated the grindability of α-case formed on cast titanium. They proposed that the ease of grindability of the α-case on c.p. Ti and Ti–6Al–4V was very similar. However, the grinding of the interior of c.p. Ti, as compared to that of Ti–6Al–4V, was more difficult because of its higher ductility. On the other hand, if current titanium prostheses are fabricated by CAD/CAM, the alloys can be fabricated by using a graphite or copper mold instead of a dental investment mold.

Results and discussion

Characterization of microstructures

The microstructures of the etched Ti–Sn alloys are shown in Fig. 1. The microstructures of Ti–1Sn and Ti–5Sn were

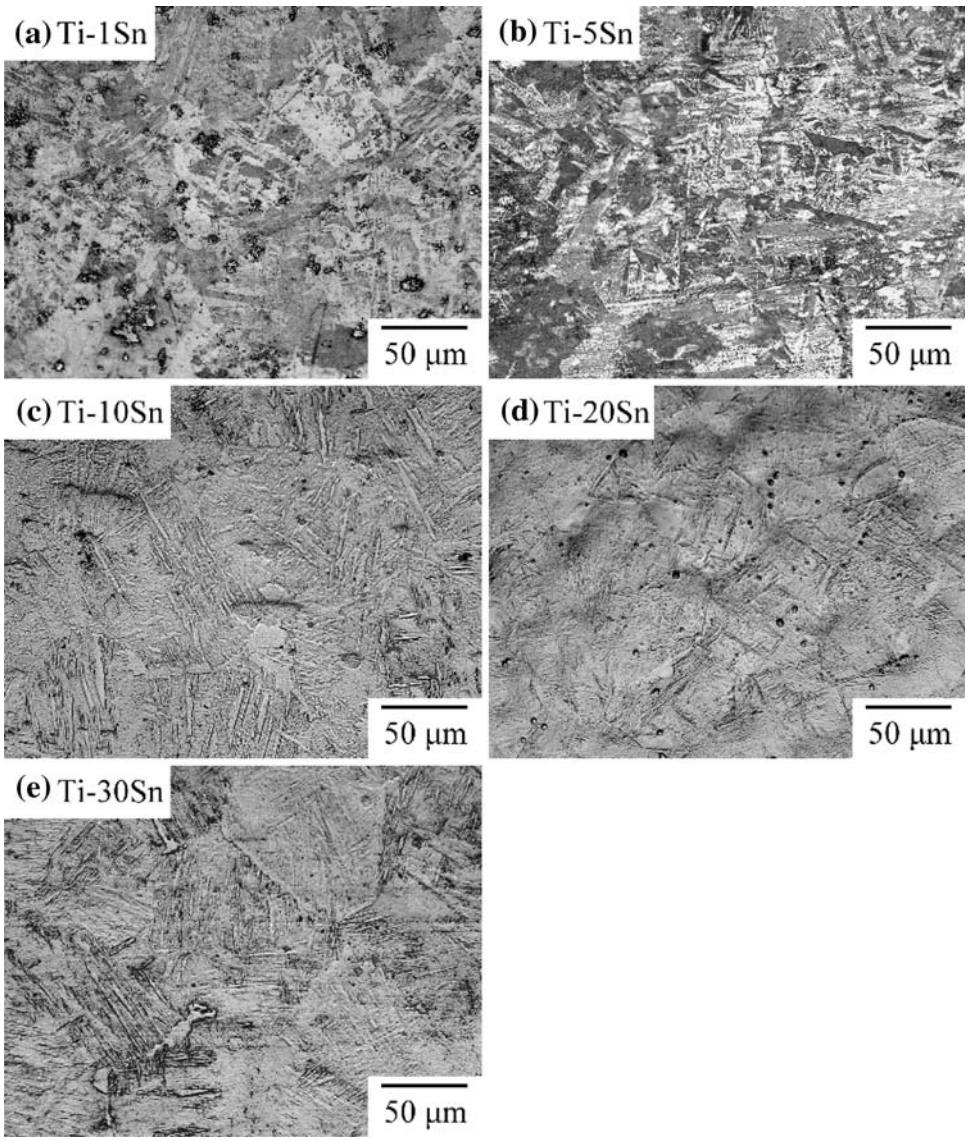

Fig. 1 Optical micrographs of the etched Ti–Sn alloys showing martensitic structures of the α phase **a** Ti–1Sn, **b** Ti–5Sn, **c** Ti–10Sn, **d** Ti–20Sn and **e** Ti–30Sn

different from the other Ti–Sn alloys containing greater Sn content. The Ti–1Sn and Ti–5Sn exhibited a feather-like microstructure similar to the typical morphology of c.p. Ti. When the Sn content was 10 wt% and greater, the fine, acicular martensitic structure of the α' phase was observed. A similar phenomenon was also seen in the Ti–Zr alloy system [13]. The XRD results indicated that the diffraction peaks of all the Ti–Sn alloys matched in the α' phase [21]. There was no indication that β phase peaks or any intermediate phases were included in any of the diffraction patterns obtained, which is different from the phases expected from the equilibrium phase diagram. In general, the phases of as-cast alloys related closely to the cooling rate [25, 26]. If the cooling rate from the β-region is sufficiently rapid, martensitic structure α phase is formed, or the β phase is retained. Accordingly, no peaks corresponding to intermetallic compound were detected in any of our specimens. Moreover, the cooling rates in the commercial casting systems are generally sufficient to cause these transformations of Ti alloys. The similar results can be found in our previous reports in Ti–Cr alloys [11]. In addition, Sato et al. [27] measured the martensitic transformation ($\beta \rightarrow \alpha'$) start temperature (Ms) and showed that in the range 2–9 at.% Sn, Ms is 740–760°C. This could partially explain why all the Ti–Sn alloys exhibit α' phase. As a result, the as-cast Ti–Sn alloys with Sn contents ranging from 1 to 30% consisted of α' phase due to nonequilibrium cooling.

Microhardness

Figure 2 shows the microhardness values of the Ti–Sn alloys. The hardness of c.p. Ti was 186 HV. The hardness of the Ti–Sn alloys increased as the Sn content increased in a range between 246 HV (Ti–1Sn) and 357 HV (Ti–30Sn). Except for Ti–1Sn and Ti–5Sn, the ANOVA results showed significant differences among the microhardness values for c.p. Ti and Ti–Sn alloys ($p < 0.05$). All the Ti–Sn alloys had significantly greater ($p < 0.05$) hardness than the c.p. Ti tested. Since the Ti–Sn alloys exhibited a single α phase in this study, their hardness values showed continuous change throughout the system due to solid-solution hardening in the α phase. Of the Ti–Sn alloys, the alloy with 30 wt% Sn content exhibited the highest hardness value.

Grindability

The grinding rates of the Ti–Sn alloys at four different speeds are shown in Fig. 3. Up to 1200 m/min, the grinding rates of Ti–10Sn, Ti–20Sn, and Ti–30Sn tended to increase with the speed. However, the grinding rates of Ti–1Sn, Ti–5Sn, and c.p. Ti tended to increase at higher speed but decreased at 1200 m/min. At 500 m/min, the grinding rates for the Ti–20Sn alloy were significantly higher than those of the other metals tested ($p < 0.05$); moreover, the rate for Ti–20Sn was about twice that of c.p. Ti. Furthermore, at 1200 m/min, the rates for Ti–20Sn were also higher than those for the other Ti–Sn alloys tested. It is noteworthy that the grinding rate of Ti–20Sn at 1200 m/min was about 4 times that of c.p. Ti. The results of Duncan's multiple comparison test revealed that the grinding rate of Ti–20Sn was significantly ($p < 0.05$) higher than those for Ti–1Sn, Ti–5Sn, and c.p. Ti at 1200 m/min; however, there were no significant differences among the rates for Ti–10Sn, Ti–20Sn, and Ti–30Sn.

The grinding ratios of the Ti–Sn alloys are shown in Fig. 4. Except for c.p. Ti, the ratios of all the Ti–Sn alloys

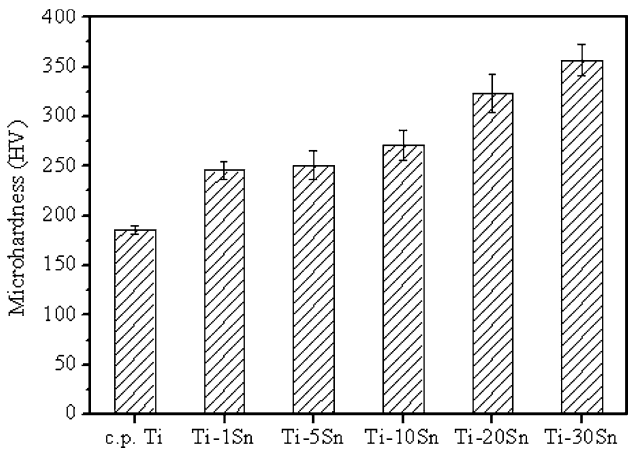

Fig. 2 Microhardness of as-cast Ti–Sn alloys compared with that of c.p. Ti. The microhardness of Ti–Sn alloys are greater than that of c.p. Ti, and increased as the Sn content increased

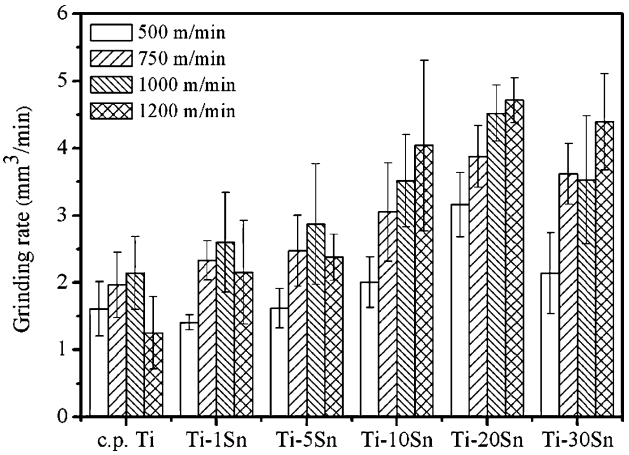

Fig. 3 Grinding rates of c.p. Ti and Ti–Sn alloys at four different speeds. The Ti–Sn alloys had greater grinding rates than that of c.p. Ti, especially for Ti–10Sn, Ti–20Sn, and Ti–30Sn at higher grinding speeds

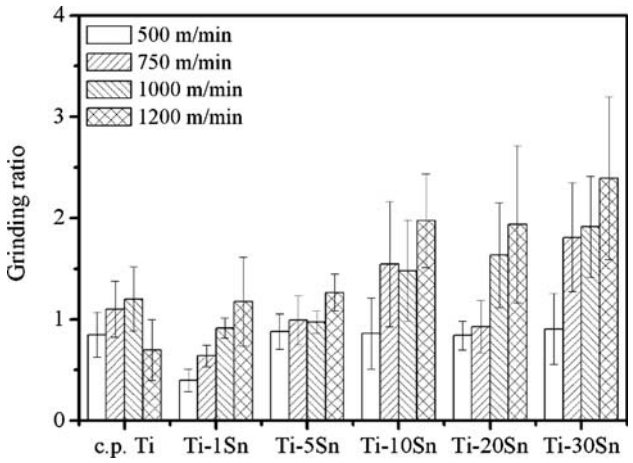

Fig. 4 Grinding ratios of c.p. Ti and Ti–Sn alloys at four different speeds. The grinding ratios of Ti–10Sn, Ti–20Sn, and Ti–30Sn are greater at higher grinding speeds, which signify lower tool wear for the same volume of metal removed

tended to increase as the speed increased to 1200 m/min. At 1200 m/min, all the alloys exhibited a significantly higher ratio than did the c.p. Ti ($p < 0.05$). It is noteworthy that the ratios for Ti–10Sn, Ti–20Sn, and Ti–30Sn at 1200 m/min were about 2.8, 2.7, and 3.4 times that for the c.p. Ti, respectively. Moreover, at 1000 m/min, Ti–20Sn and Ti–30Sn had a significantly higher ratio than did the c.p. Ti ($p < 0.05$). The ratios of Ti–20Sn and Ti–30Sn at 1000 m/min were about 1.4 and 1.6 times that of the c.p. Ti, respectively. Tool life can be predicted on the basis of an evaluation of the grinding ratio. Thus, a higher ratio signifies lower tool wear for the same volume of metal removed [10]. The ratios varied widely for the metals tested, probably because the losses in the volumes of both the ground metal and the wheel material were very small.

Although the measurements were straightforward, the interpretation of the mechanism for the measured grindability values could be quite complex. Such effects as composition, hardness, strength, modulus, ductility, and crystal structure/phase could all affect the grindability of the alloy. Takeyama [28] demonstrated that greater strength and hardness of a material generally render the machining thereof more difficult. However, in our study, the Ti–Sn alloys had greater hardness values than that of c.p. Ti, but they also had higher grinding rates, especially for Ti–10Sn, Ti–20Sn, and Ti–30Sn. In earlier studies [29–31], the respective researchers discussed grindability in terms of the hardness of the metals. Nevertheless, in this study there appeared to be no correlation between the loss in volume and the hardness of the metals. This result also agrees with that reported by Ohkubo et al. [23], who tested c.p. Ti and the Ti–6Al–4V alloy. In fact, it appears that hardness is not among the principal reasons for better grindability. Therefore, the exact mechanisms affecting the grindability of various alloys are complex and thus merit further study.

It is known that lower ductility is generally beneficial to the grindability of metals [32]. In our previous study [21], three-point bending tests were performed to evaluate the

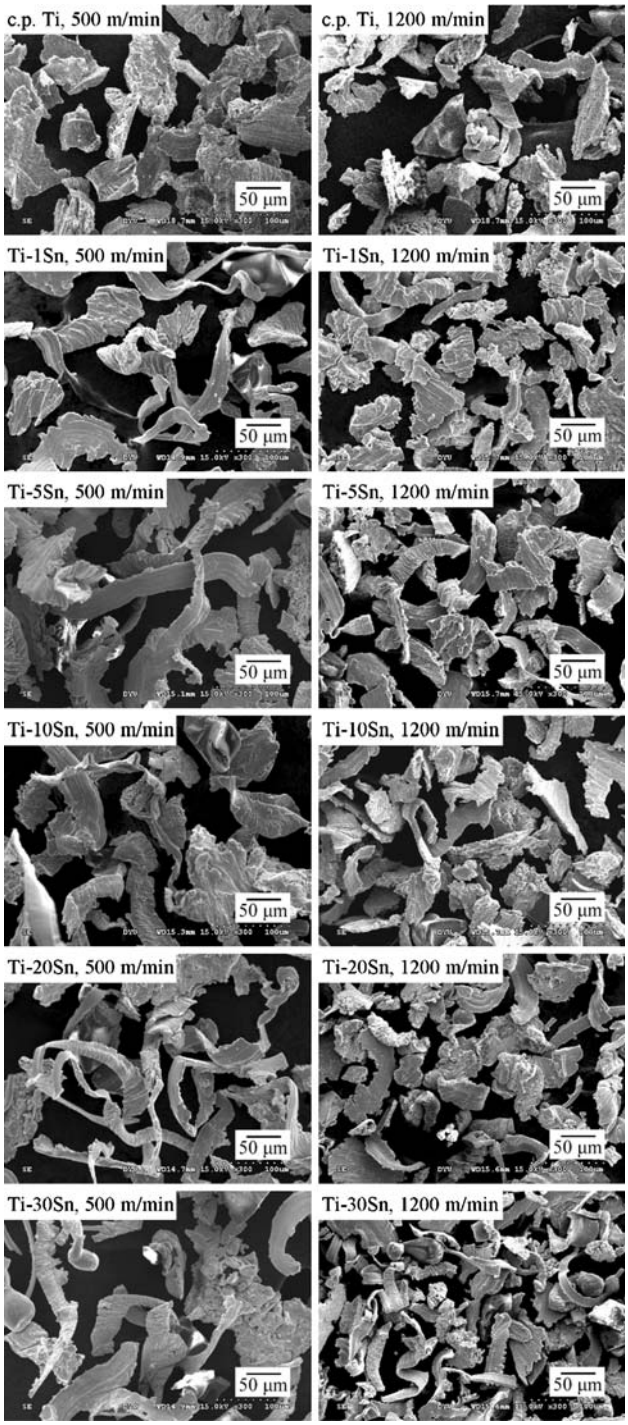

Fig. 5 SEM micrographs of metal chips of c.p. Ti and Ti–Sn alloys from grinding at 500 (*left side*) and 1200 (*right side*) m/min. The size of the metal chips at 500 m/min generally appeared somewhat larger than those at 1200 m/min

mechanical properties of Ti–Sn alloys. The results indicated that when the Sn content was 20% or greater, the alloys showed decreasing ductility. In this study, the magnitudes of grinding rate and ratio for Ti–10Sn, Ti–20Sn, and Ti–30Sn were much higher than those for c.p. Ti and the other Ti–Sn alloys. The reduced ductility (lower bending deflection) was considered to be a primary contributing factor to the increased grindability.

Observation of metal chips and ground surfaces

Typical metal chips resulting from grinding at 500 and 1200 m/min are shown in Fig. 5. Although no quantitative analysis was performed, the size of the metal chips of c.p. Ti and Ti–Sn alloys at 500 m/min generally appeared somewhat larger than those at 1200 m/min. It seems that the display of finer metal chips is one property that exhibits better grindability. This result can also be found in many as-cast Ti alloy systems [2, 8, 11, 12]. Furthermore, several long chips were observed, particularly at 500 m/min. Moreover, there were no clear differences in the appearance of the metal chips among the c.p. Ti and the Ti–Sn alloys.

Figure 6 shows optical micrographs of the ground surfaces of the metals at 500 and 1200 m/min. Grinding marks were observed on all the metals at all speeds. There were no pronounced differences in the appearance of the ground surfaces among the Ti–Sn alloys at 500 m/min, except for a few adhesion marks on the ground surface of the c.p. Ti. Grinding adhesion of metal was observed to a greater degree for the c.p. Ti, Ti–1Sn and Ti–5Sn alloys ground at 1200 m/min. Additionally, grinding burns were found on the c.p. Ti, Ti–1Sn and Ti–5Sn alloys at 1200 m/min. As mentioned in the literature [2, 9], the grinding burns typically found on titanium and its alloys result from high-speed grinding. Moreover, appreciable sparking was occasionally observed during the grinding test, especially at high speeds, a phenomenon attributable to the grinding heat and metal powder. The grinding temperature increased with the speed. Additionally, changes in the grinding state, likely caused by the clogging of the wheel from ground metal, were observed. The occurrence of adhesion of metal on the wheel surface could result in a decrease in grinding rate. Moreover, the adhesion caused filling of the pores of the grinding wheel and obstructed self-dressing of the wheel. The changes could be easily assessed by the decrease in the grinding sound or the interruption of grinding sparks. Similar results were also found for Ti–Au and Ti–Zr alloys [2, 13, 33].

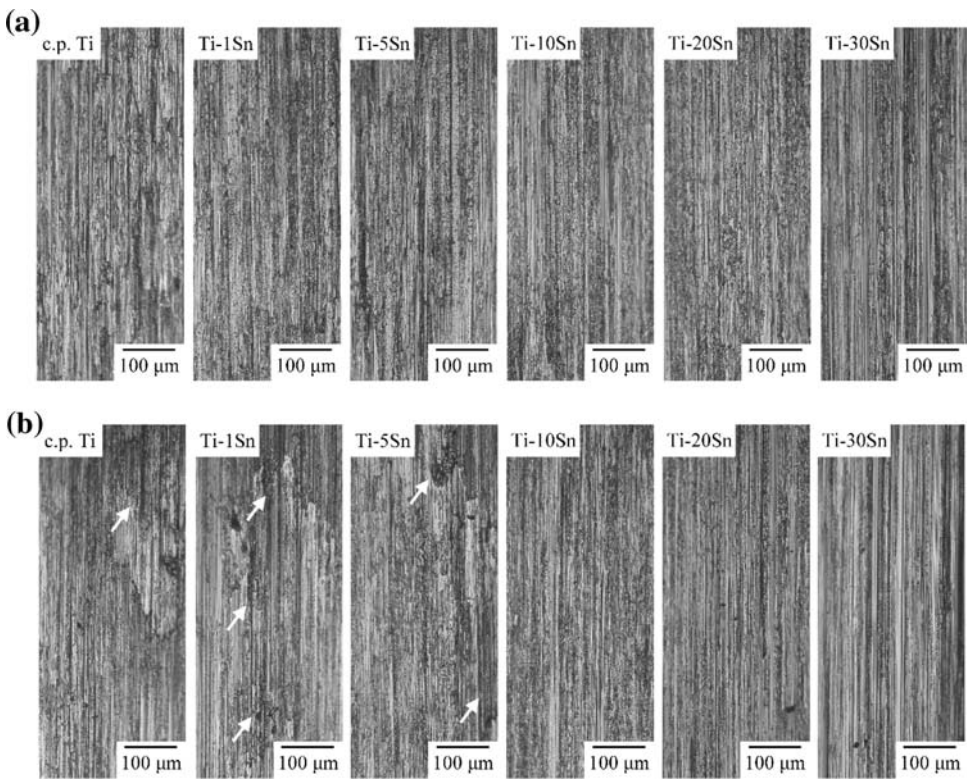

Fig. 6 Grinding surfaces of c.p. Ti and Ti–Sn alloys after grinding test at **a** 500 and **b** 1200 m/min. Grinding burn (*arrow* symbol) refers to discoloration of the specimen surface caused by the heat of grinding

Conclusions

1. On the basis of the results of XRD and optical microscopy, all the Ti–Sn alloys exhibited hcp α structures.
2. At a grinding speed of 500 m/min, the rates for Ti–20Sn were notably higher than those for the other metals tested; moreover, the grinding rate of Ti–20Sn was about 2 times that of c.p. Ti. However, at the higher speed of 1200 m/min, the rate for Ti–20Sn was also higher than the rates for the other alloys tested and about 4 times that for c.p. Ti.
3. The grinding ratios of Ti–10Sn, Ti–20Sn and Ti–30Sn at 1000 m/min and greater were noticeably higher than for all other metals at all speeds. It is notable that the grinding ratio for Ti–30Sn at 1200 m/min was almost 3.4 times that for c.p. Ti.

Acknowledgements The authors acknowledge the partial financial support of National Science Council of Taiwan (NSC 97-2221-E-212-009 and NSC 98-2221-E-212-013). The authors also express appreciation to Dr. Cheryl Rutledge, Associate Professor of English, Da-Yeh University, for her editorial assistance.

References

1. Oshida Y (2007) Bioscience and bioengineering of titanium materials. Elsevier, Oxford, p 3
2. Takahashi M, Kikuchi M, Okuno O (2004) Dent Mater J 23:203
3. Okuno O, Hamanaka H (1989) Dent Jpn 26:101
4. Lautenschlager EP, Monaghan P (1993) Int Dent J 43:245
5. Takahashi M, Kikuchi M, Takada Y, Okuno O (2002) Dent Mater J 21:270
6. Duret F, Blouin JL, Duret B (1988) J Am Dent Assoc 117:715
7. Craig RG (2006) Restorative dental materials, 12th edn. CV Mosby, St. Louis, p 454
8. Kikuchi M, Takada Y, Kiyosue S, Yoda M, Woldu M, Cai Z, Okuno O, Okabe T (2003) Dent Mater 19:375
9. Kikuchi M, Takahashi M, Okuno O (2003) Dent Mater J 22:328
10. Kikuchi M, Takahashi M, Sato H, Okuno O, Nunn ME, Okabe T (2005) J Biomed Mater Res B Appl Biomater 77:34
11. Hsu HC, Wu SC, Chiang TY, Ho WF (2009) J Alloys Compd 476:817
12. Hsu HC, Pan CH, Wu SC, Ho WF (2009) J Alloys Compd 474:578
13. Ho WF, Chen WK, Wu SC, Hsu HC (2008) J Mater Sci Mater Med 19:3179
14. Ho WF, Cheng CH, Pan CH, Wu SC, Hsu HC (2009) Mater Sci Eng C 29:36
15. Walker PR, LeBlanc J, Sikorska M (1989) Biochemistry 28:3911
16. Rao S, Ushida T, Tateishi T, Okazaki Y, Asao S (1996) Biomed Mater Eng 6:79
17. Davidson JA, Mishra AK, Kovacs P, Poggie RA (1994) Biomed Mater Eng 4:231
18. Grimme P, Hupfer P (1992) Metallurgy 46:365
19. Niinomi M (2003) Sci Tech Adv Mater 4:445
20. Niinomi M (2002) Metall Mater Trans 33A:477
21. Hsu HC, Wu SC, Hong YS, Ho WF (2009) J Alloy Compd 479:390
22. Watanabe I, Ohkubo C, Ford JP, Atsuta M, Okabe T (2000) Dent Mater 16:420
23. Ohkubo C, Watanabe I, Ford JP, Nakajima H, Hosoi T, Okabe T (2000) Biomaterials 21:421
24. Koike M, Jacobson D, Chan KS, Okabe T (2009) Dent Mater J 28:587
25. Huang YC, Suzuki S, Kaneko H, Sato T (1970) The science, technology and application of titanium. Pergamon Press, Oxford, p 691, 695
26. Williams JC (1973) Titanium science and technology, metallurgical society of AIME. Plenum Press, New York, p 1433
27. Sato T, Hukai S, Huang YC (1960) J Aust Inst Met 5:149
28. Takeyama H, Yoshikawa T, Takada T (1975) J Jpn Soc Preci Eng 41:392
29. Grajower R, Kurz I, Bapna MS (1986) Dent Mater 2:187
30. Reisbick MH, Bunshah RF (1973) J Dent Res 52:1138
31. O'Brien WJ (1989) Dental materials: properties and selection, third edn. Quintessence, Chicago, p 515
32. Okabe T, Kikuchi M, Ohkubo C, Koike M, Okuno O, Oda Y (2004) J Miner Met Mater Soc 56:46
33. Takahashi M, Kikuchi M, Okuno O (2009) Mater Trans 50:859